Neuron, Vol. 31, 617–630, August 30, 2001, Copyright ©2001 by Cell Press

The *C. elegans* Glutamate Receptor Subunit NMR-1 Is Required for Slow NMDA-Activated Currents that Regulate Reversal Frequency during Locomotion

Penelope J. Brockie, Jerry E. Mellem, Thomas Hills, David M. Madsen, and Andres V. Maricq[1]
Department of Biology
University of Utah
Salt Lake City, Utah 84112

Summary

The *N*-methyl-D-aspartate (NMDA) subtype of glutamate receptor is important for synaptic plasticity and nervous system development and function. We have used genetic and electrophysiological methods to demonstrate that NMR-1, a *Caenorhabditis elegans* NMDA-type ionotropic glutamate receptor subunit, plays a role in the control of movement and foraging behavior. *nmr-1* mutants show a lower probability of switching from forward to backward movement and a reduced ability to navigate a complex environment. Electrical recordings from the interneuron AVA show that NMDA-dependent currents are selectively disrupted in *nmr-1* mutants. We also show that a slowly desensitizing variant of a non-NMDA receptor can rescue the *nmr-1* mutant phenotype. We propose that NMDA receptors in *C. elegans* provide long-lived currents that modulate the frequency of movement reversals during foraging behavior.

Introduction

N-methyl-D-aspartate (NMDA) receptors, a subset of ionotropic glutamate receptors, play diverse roles in the nervous system, including regulation of synaptic development and function, the refinement of synaptic connections with experience, and synaptic plasticity and learning (Dingledine et al., 1999). Named for their activation by the selective agonist NMDA, these receptors are widely expressed in the central nervous system of vertebrates. Two characteristics distinguish NMDA receptors from the larger class of non-NMDA receptors. First, NMDA receptors can act as neuronal coincidence detectors. Thus, the opening of NMDA receptors requires both glutamate binding to the receptor and concurrent depolarization of the membrane. Current evidence suggests that NMDA receptors are required for neuronal responses to correlated synaptic inputs and may play a key role in extracting information from sensory inputs (Bourne and Nicoll, 1993; Harsch and Robinson, 2000; Stevens and Zador, 1998). Coincidence detection is also thought to play a prominent role in the changes in synaptic strength observed in cellular models of learning and memory such as long-term depression and potentiation (LTD and LTP, respectively) (Malenka and Nicoll, 1999; Malinow et al., 2000). In support of their role in synaptic plasticity, targeted disruption of NMDA receptors in the hippocampus of mice interferes with spatial learning (Tsien et al., 1996), whereas overexpression of the NMDA receptor subunit NR2B increases LTP and performance in behavioral tasks (Tang et al., 1999).

A second characteristic that distinguishes NMDA receptors from the non-NMDA subtypes is their slow kinetics. Thus, activation of NMDA receptors results in long-lived currents that may promote rhythmic activity, such as in spinal cord neurons that control locomotion in lamprey (Sigvardt et al., 1985), amphibia (Sillar and Simmers, 1994), and mammals (Schmidt et al., 1998). The time course of currents mediated by NMDA receptors may also facilitate spatiotemporal integration of sensory inputs (Viana Di Prisco et al., 1995). In particular, one role for NMDA receptors in the retina depends on its slow rate of desensitization. By providing a maintained current response to glutamate that acts in concert with the rapidly desensitizing currents mediated by non-NMDA receptors, NMDA receptors participate in the synaptic transfer of graded photoresponses from bipolar to ganglion cells (Matsui et al., 1998; Taylor et al., 1995).

A large variety of NMDA receptor subtypes, each with distinguishing features, participates in neural circuits throughout the central nervous system. Because pharmacological tools are likely to target a variety of NMDA receptor subtypes, it is difficult to address how a particular NMDA receptor subunit contributes to the function of a specific neural circuit. To address this question, we have undertaken a genetic and electrophysiological approach to investigate how NMDA receptors contribute to synaptic function in *Caenorhabditis elegans*. By analyzing patterns of locomotion in mutant backgrounds, we can determine which properties of the NMDA receptor are required for the processing of sensory information. *C. elegans* has a well-described nervous system, and many of the neurons that control or drive locomotion have been identified (White et al., 1986). Under laboratory conditions, worms move primarily in the forward direction punctuated by brief backward movements (Croll, 1975). The locomotory control circuit that controls these reversals of movement was first described in relationship to the worm's response to tactile stimulation (Chalfie et al., 1985; White et al., 1986). Three interneurons, AVA, AVD, and AVE, are required for the backing escape response, and two interneurons, AVB and PVC, mediate the forward escape response. A non-NMDA ionotropic glutamate receptor, GLR-1, is expressed in these interneurons and is required for a backing response to tactile stimulation to the worm's nose (Hart et al., 1995; Maricq et al., 1995). Also, expression of a dominantly active glutamate receptor in these same interneurons showed that the circuit functions in a distributed manner to control the duration of forward and backward movement (Zheng et al., 1999).

Here we show that *nmr-1* encodes a glutamate receptor subunit with greatest sequence identity to vertebrate NR1 NMDA receptor subunits. NMR-1 is expressed in the interneurons of the locomotory control circuit. From the AVA interneuron, we recorded NMDA-activated ionic

[1]Correspondence: maricq@biology.utah.edu

currents that are dependent on NMR-1. We also show that NMR-1 is localized to punctate structures in the processes of these neurons and that localization may be dependent on a PDZ domain binding motif at the C terminus of NMR-1. By generating a null mutation in *nmr-1*, we show that it is required for the regulation of the duration of forward movement that is important during foraging behavior. The mutant phenotype can be rescued by expressing a slowly desensitizing mutant variant of GLR-1 in transgenic mutants, indicating that the slow kinetics of NMDA-dependent currents are crucial for NMR-1 function. We also find that the localization and function of the non-NMDA receptor subunit GLR-1 are not dependent on NMR-1. Together, our findings suggest that NMR-1 regulates locomotion by contributing to the switch from forward to backward movement.

Results

nmr-1 Encodes an NMDA Receptor that Is Expressed in Interneurons

We identified a full-length cDNA that is predicted to encode a 1025 amino acid polypeptide that shows greatest identity to NR1 subunits of the NMDA receptor family (Figure 1). The topological arrangement is similar to that of other NMDA and non-NMDA receptors and includes four hydrophobic regions predicted to be three transmembrane regions and a pore-forming region (Dingledine et al., 1999). Like other glutamate receptors, two separated regions in the protein have a strong identity to bacterial periplasmic binding proteins and are required for ligand binding (Kuryatov et al., 1994; SternBach et al., 1994). Another region conserved in all known ionotropic glutamate receptors is a nine-amino acid sequence (SYTANLAAF) in TMIII (Figure 1). In many glutamate receptors, the last several amino acids share identity with a consensus sequence that is required for interaction with proteins that contain PDZ domains (Kornau et al., 1997). NMR-1 has a type II PDZ domain binding motif (Songyang et al., 1997), suggesting that it may physically interact with PDZ domain proteins (Figure 1).

The pore region contains a signature feature of NMDA receptors—a conserved asparagine residue that affects divalent cation permeability (Burnashev et al., 1992). NMDA receptors are blocked by the noncompetitive antagonist MK-801, and this blockade can be disrupted by mutating a few critical amino acids, including W632, N637, and A666 (Ferrer-Montiel et al., 1995), that are conserved in *C. elegans* NMR-1. Unlike the case for non-NMDA receptors, glutamate activation of NMDA receptors requires the concomitant binding of the coagonist glycine. Amino acids important for glycine binding are also conserved in *C. elegans* NMR-1 (Figure 1) (Kuryatov et al., 1994).

To determine which cells express NMR-1, we examined transgenic strains that expressed, under the control of *nmr-1* regulatory sequences, the reporter molecule green fluorescent protein (GFP) (Chalfie et al., 1994). Expression was limited to a small subset of neurons (Brockie et al., 2001) (Figures 2A and 2B), including most of the interneurons of the locomotory control circuit (AVA, AVD, AVE, and PVC). To determine the subcellular localization of NMR-1 and to examine whether the expression pattern was dependent on intragenic regulatory regions, we generated transgenic strains that expressed a full-length GFP::NMR-1 N-terminal fusion protein. In this reporter fusion protein, GFP was inserted in frame in the extracellular domain immediately downstream of the predicted signal sequence. The fusion protein was expressed in the same subset of neurons as described for the reporter construct alone, suggesting that intragenic control elements do not play a role in directing the cell-specific expression of NMR-1. Moreover, we found that the N-terminal fusion protein was localized to clusters along the neuronal processes (Figure 2C), suggesting that it was synaptically localized (Rongo et al., 1998).

The role of PDZ domain binding motifs in NMDA receptor localization and function is presently unclear. Studies that have examined the effects of truncating the C-terminal domain of NR2 receptor subunits have found conflicting results for localization as well as function (Mori et al., 1998; Sprengel et al., 1998). To address the question of whether the PDZ domain binding motif in NMR-1 is required for localization or function, we generated a full-length NMR-1::GFP C-terminal fusion protein in which GFP was inserted in frame in the intracellular domain after the last amino acid of the predicted protein. This fusion protein was also expressed in the same subset of neurons described for the *nmr-1* reporter construct alone. Because the location at the very C terminus of the protein is essential for the function of PDZ domain binding motifs (Songyang et al., 1997), the NMR-1 C-terminal fusion to GFP was expected to disrupt the function of the motif and, therefore, interfere with PDZ domain binding. Examination of GFP expression in transgenic worms that expressed the C-terminal fusion protein showed diffused GFP expression with no apparent clustering of the GFP signal (Figure 2D). This result suggests that the type II PDZ domain binding motif is important for localization of NMR-1 to synapses, although we cannot rule out that GFP disrupts some other C-terminal-dependent protein-protein interaction.

nmr-1 Mutants Are Viable and Coordinated

Disruption of a subset of neurons in the locomotory control circuit that express NMR-1 causes severe locomotory and behavioral defects (Chalfie et al., 1985; Zheng et al., 1999). To determine the contribution of NMR-1 to the function of this circuit, we generated a deletion mutation in *nmr-1* (Figure 3A). By a process of transposon insertion followed by imprecise excision (Zwaal et al., 1993), we generated a disrupted gene that encodes a protein fragment that lacks three of the transmembrane regions, including the pore domain and the ligand binding region (Figure 3B). Worms that were homozygous for the deletion mutation (*ak4*) were viable and normal in appearance. *nmr-1(ak4)* mutants moved at normal velocity, and there were no apparent abnormalities in their spontaneous movement (Table 1). A number of sensory modalities and behaviors that are dependent on periodic contractile events, such as brood size and defecation cycle, were also unaffected in *nmr-1(ak4)* mutants (Table 1).

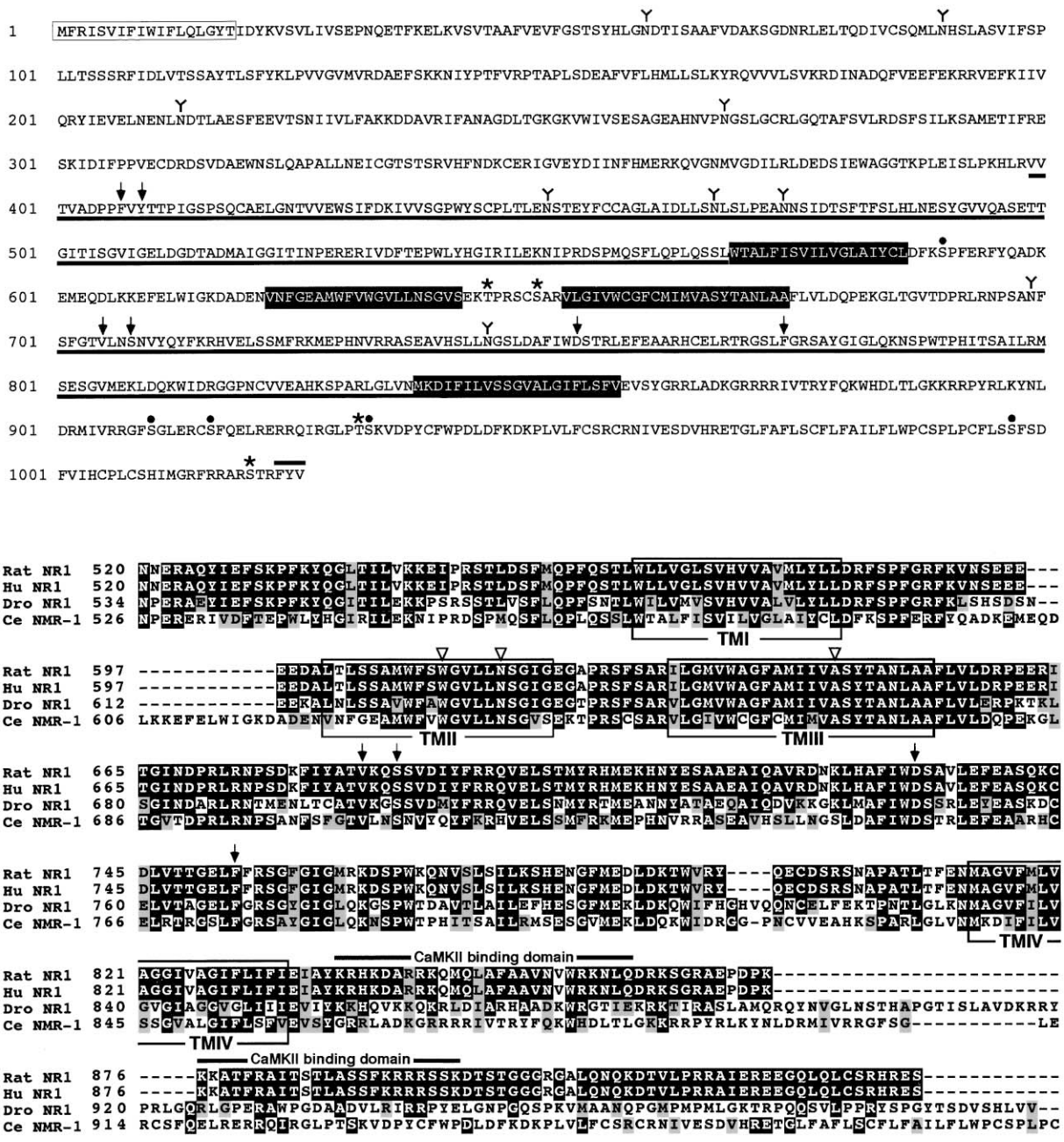

Figure 1. Predicted Amino Acid Sequence of NMR-1

(Top) Amino acids encoded by the *nmr-1* cDNA are numbered beginning with the first predicated methionine (single-letter code). The open box indicates the predicted signal sequence. Consensus *N*-linked glycosylation sites (flags), protein kinase C phosphorylation sites (asterisk), and casein kinase II phosphorylation sites (filled circles) are shown. The underlined domains indicate the regions of alignment with bacterial periplasmic protein LAOBP (Stern-Bach et al., 1994). The arrows mark residues important for binding to the coagonist glycine. Black boxes show the four hydrophobic domains. The predicted type II PDZ domain binding motif (FYV) is indicated by a bar. (Bottom) Domain organization and comparison of *C. elegans* (Ce) NMR-1 with rat, human (Hu), and *D. melanogaster* (Dro) NR1. The hydrophobic domains are outlined in black (TMI–TMIV). The arrows indicate conserved residues critical for glycine binding. Open triangles show residues required for inhibition by the antagonist MK-801 (Ferrer-Montiel et al., 1995). This includes the conserved asparagine found in TMII of NMDA subunits that facilitates the voltage dependent Mg^{2+} blockade. Two domains that have been shown to bind to CaMKII are indicated. The cDNA sequence differs from that predicted by GENEFINDER analysis of F07F6 (Wilson et al., 1994).

Sensory input, whether mechanical or chemical, ultimately causes a change in either the direction or speed of locomotion in *C. elegans*. In *nmr-1* mutants, the coordination of movement and speed of locomotion were normal, as were the locomotory responses to specific sensory inputs. These sensory stimuli may not appropri-

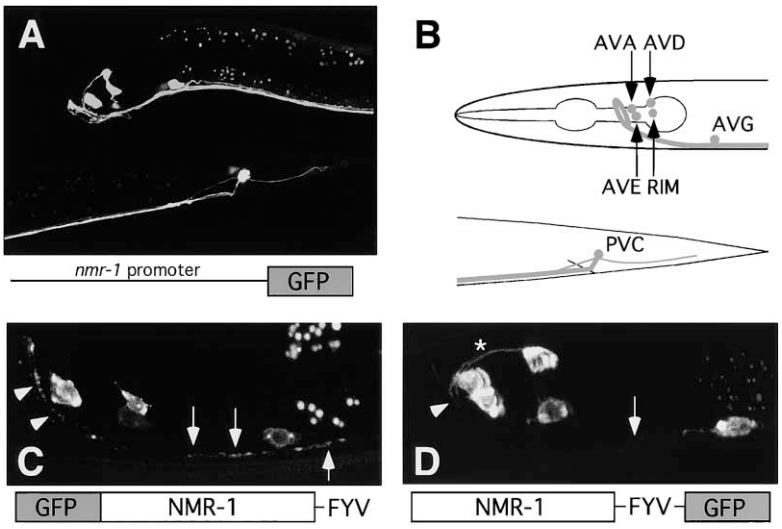

Figure 2. N-terminal GFP::NMR-1 Fusion Protein Appears Localized at Synapses

Approximately 5 kb of *nmr-1* 5′ untranslated sequence fused to GFP was used to show expression of *nmr-1* in a small subset of neurons.

(A and B) A confocal image (A) and schematic representation (B) of a transgenic worm that expressed the *nmr-1::GFP* promoter fusion. Anterior regions are shown on top and posterior regions on the bottom.

(C) A transgenic worm that expressed an N-terminal GFP::NMR-1 fusion protein where GFP was fused immediately after the signal sequence. A punctate pattern of expression was observed in the neural processes of the nerve ring (arrowheads) and ventral cord (arrows), suggesting that the fusion protein was localized to synapses.

(D) A transgenic worm that expressed a C-terminal NMR-1::GFP fusion protein. Although difficult to see, no puncta were observed in the processes of either the nerve ring (arrowhead) or ventral cord (arrow). The diffuse distribution of NMR-1::GFP was most evident in the process of the AVD interneuron (asterisk).

ately mimic the complex sensory inputs received by the worm as it forages. To analyze further the role of *nmr-1* in the control of locomotion, we tested whether the deletion in *nmr-1* altered locomotion while the worm explored its environment.

NMR-1 Regulates the Probability of Backward Locomotion

Wild-type worms modulate the duration and direction of their movements in a context-dependent manner—presumably as part of a foraging strategy for food (Croll, 1975). Using a video camera to track worms on food-free agar plates, we monitored their distribution of turning angles (Figures 4A and 4B). Compared with wild-type worms, *nmr-1(ak4)* mutants had fewer high-angle turns. This defect was rescued in transgenic *nmr-1(ak4)* mutants that expressed a genomic *nmr-1* clone. By recording the duration of each forward and backward movement, we showed that the decrease in high-angle turns in *nmr-1(ak4)* mutants was due to fewer spontaneous reversals in the direction of movement.

On food-free agar plates, wild-type worms moved forward on average approximately 25 s before reversing and moving backward. In contrast, *nmr-1(ak4)* mutants did not modulate their direction of movement as often and moved forward about twice as long before reversing (Figure 4C). The altered duration of locomotion could be rescued in transgenic *nmr-1(ak4)* mutants that expressed a wild-type genomic *nmr-1* clone. A frame-shifted version of this clone that introduced an early stop codon did not rescue the movement phenotype, establishing that rescue was dependent on the expression of NMR-1. To address whether rescue of the locomotory defect was also dependent on localization of NMR-1, we examined transgenic *nmr-1(ak4)* mutants that expressed full-length fusion proteins with GFP. The localized, N-terminal GFP::NMR-1 fusion protein fully rescued the movement phenotype (Figure 4C). Although expression levels of the protein were approximately equivalent (Figure 2), only partial rescue was observed with the C-terminal NMR-1::GFP fusion protein, suggesting that appropriate localization of NMR-1 is important for its function in the locomotory control circuit.

Because glutamatergic signaling to the command interneurons is required for the initiation of some backward movements, for example, the nose touch response, one might expect that mutations that disrupt sensory input to these neurons would lower the probability of moving backward. To test this hypothesis, we examined the behavior of *glr-1(ky176)* mutants and the double mutant *nmr-1(ak4);glr-1(ky176)*. GLR-1 is required in the interneurons for the backward avoidance response to tactile stimulation to the nose (Hart et al., 1995; Maricq et al., 1995), and its deletion might reduce the probability of backward movement during foraging behavior. As expected, compared with wild-type worms, the duration of forward movement was increased in *glr-1(ky176)* mutants. This result suggests that "spontaneous" reversals are influenced by sensory stimulation. Interestingly, we observed an additive effect on backward probability in the double mutant. *nmr-1(ak4);glr-1(ky176)* mutants moved forward for an average of about 125 s, far longer than for either single mutant (Figure 4D). This suggests that a parallel sensory pathway, independent of GLR-1, contributes to backward movement. In summary, although we found that NMR-1 is not required for detection of sensory stimuli such as nose touch, it does play a major role in modulating the probability of moving backward. Thus, NMR-1 indirectly controls the direction of movement and contributes to foraging behavior in *C. elegans*.

Spontaneous Locomotion Can Be Modeled as a Random Process with Exponentially Distributed Forward Times

How do worms reverse direction in a uniform environment devoid of known sensory stimuli? One can imagine

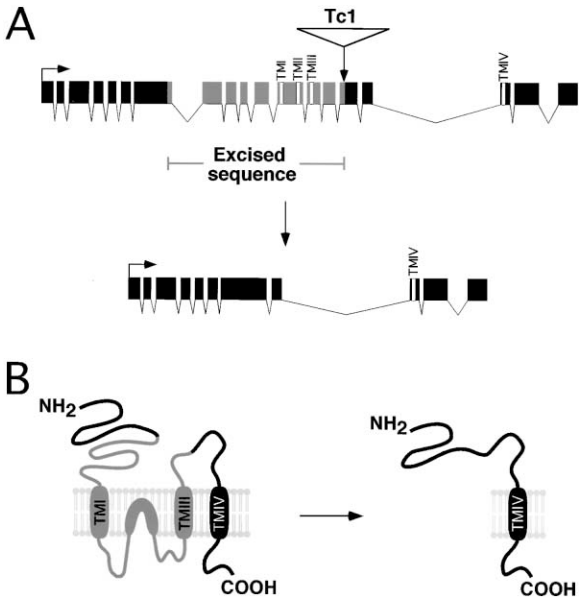

Figure 3. *nmr-1(ak4)* Deletion Mutation Removes Sequences Predicted to Encode Ligand Binding Domains and the Pore-Forming Region

(A) Genomic organization of both wild-type *nmr-1* (top) and *nmr-1(ak4)* (bottom) loci. Exons are indicated by boxes and introns by the lines between the exons. The regions predicted to encode hydrophobic domains are labeled (TMI–TMIV). The insertion site of the Tc1 transposon is indicated by the arrow. The 1.9 kb deletion generated by the imprecise excision of Tc1 is shown in gray.

(B) The predicted membrane topology of molecules encoded by wild-type *nmr-1* (left) and the *nmr-1(ak4)* deletion allele (right). Gray indicates the region eliminated by the genomic deletion and includes extracellular ligand binding domains and the pore-forming region (TMII).

at least two mechanisms that direct backward movement. First, although the agar surface on which the worms move is devoid of food, randomly distributed microscopic irregularities might be expected to provide a low level of sensory input that on occasion would be sufficient to trigger a backward movement. Second, intrinsic clock-like switching activity might contribute to the generation of periodic backward movement. To test the relative contributions of these processes, we examined the distribution of durations of forward movement (forward times). If random sensory input were contributing to the backward movement, we would expect that the distribution of forward times would be described by an exponential probability density. If, instead, the probability of moving backward was regulated by an internal clock, then the distribution of forward times should approximate a Gaussian distribution.

We found that in both wild-type worms and *nmr-1* mutants, the distribution of forward times is well fit by an exponential probability density. In *nmr-1* mutants, the time constants of the distribution are significantly longer than observed in wild-type worms (Figure 4E). This increase would occur if the probability of moving backward were randomly decreased in *nmr-1* mutants. In this case, the mean forward time should increase, and, to a first approximation, the ratio of the standard deviation to the mean should remain equal to one. We found that the mean forward time increases in *nmr-1* mutants, but the ratio of the standard deviation to mean remains constant and approximately equals one. This indicates that changing the rate of backward movement does not alter the underlying pattern of movement. The ratio of standard deviation to mean is slightly less than expected for *glr-1* mutants and is far less than expected for the *nmr-1;glr-1* double mutants (Figure 4F). These results suggest that the disruption of both GLR-1 and NMR-1 interferes with either the detection or processing of multiple sensory inputs and reveals a slower and more periodic intrinsic switching activity.

Navigation of a Maze Is Disrupted by Deletion of *nmr-1*

How might increasing the mean duration of forward movement impact a worm's ability to forage for food successfully? In order to chemotax toward a target, worms correct errors in their trajectory of movement by halting their forward movement, moving backward for a few seconds, and then redirecting their forward movement (Croll, 1975; Pierce-Shimomura et al., 1999). *nmr-1(ak4)* mutants move backward less frequently and, therefore, may be hampered in their ability to change their direction of movement. To test this possibility, we developed an assay that required worms to respond to complex cues to reach an attractive target. A simple

Table 1. Behavioral Analysis of *nmr-1*(*ak4*)

Genotype	Wild-type	*nmr-1*(*ak4*)
Nose Touch (% response)	85.0 ± 2.7 (14)	83.6 ± 2.0 (14)
Anterior Body Touch (Body bends)	1.9 ± 0.16 (12)	1.9 ± 0.21 (12)
Osmotic Avoidance (% escaped)	21.8 ± 4.0 (11)	17.8 ± 4.7 (11)
Chemotaxis to diacetyl 1:1000 (C.I.)	0.86 ± 0.04 (7)	0.87 ± 0.03 (7)
Chemotixis to diacetyl 1:10,000 (C.I.)	0.76 ± 0.02 (8)	0.80 ± 0.03 (8)
$CuSO_4$ Avoidance 100 mM (% escaped)	17.3 ± 3.0 (13)	21.9 ± 4.3 (13)
$CuSO_4$ Avoidance 200 mM (% escaped)	11 ± 3.3 (5)	16 ± 5.8 (5)
Velocity (Body bends/min)	32.2 ± 0.9 (9)	29.9 ± 0.9 (10)
Defecation cycle (Seconds)	50.5 ± 1.2 (12)	51.3 ± 1.9 (12)
Brood size (Progeny/worm)	292.3 ± 9.9 (15)	278.8 ± 5.9 (13)

Behaviors were assayed as described (see Experimental Procedures). *nmr-1*(*ak4*) worms showed no obvious behavioral defects. They responded normally to nose touch stimuli (*glr-1*[*n2461*] worms: 9.1% ± 2.5 [11]), anterior body touch, osmotic stimuli, the volatile attractant diacetyl at either a 1:1000 or 1:10,000 dilution, (C.I. = Chemotaxis Index), and the repellant $CuSO_4$ (100 or 200 mM). They also had a normal velocity of movement, duration of the defecation cycle, and brood size. Data order are mean, SEM and (n).

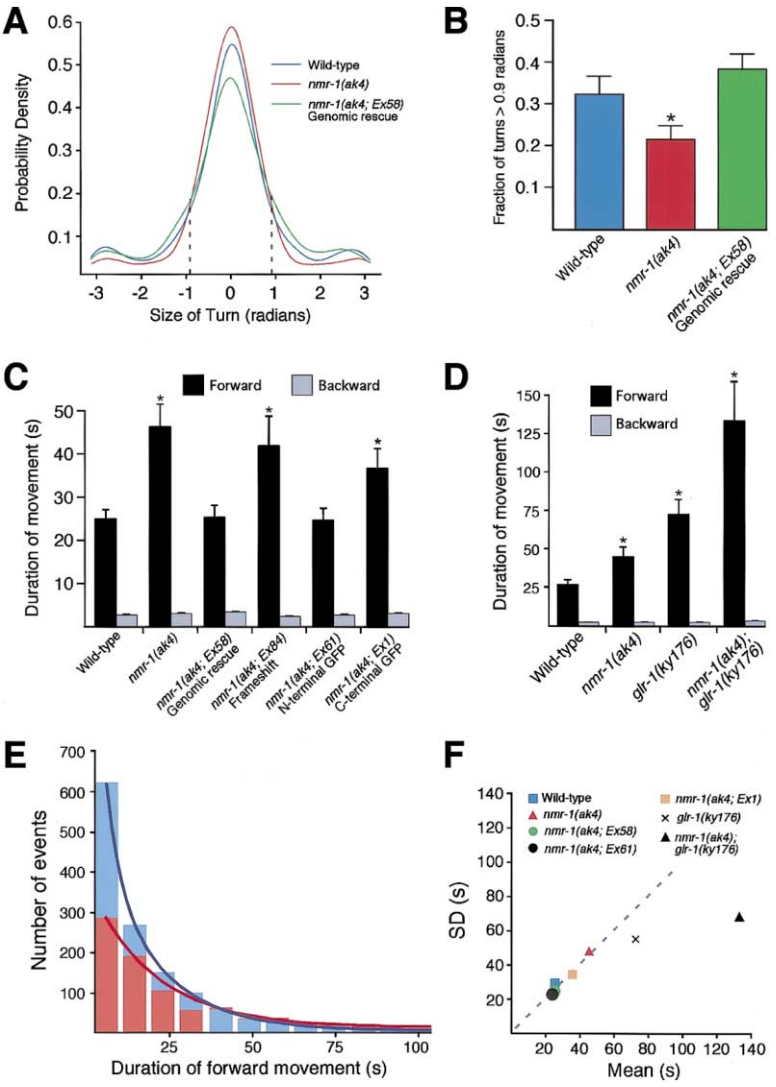

Figure 4. *nmr-1(ak4)* Mutants Show Defects in the Initiation of Backward Movements

(A) The distribution of turn angles on a food-free agar plate in wild-type worms (blue), *nmr-1(ak4)* mutants (red), and *nmr-1(ak4; Ex58)* transgenic mutants that expressed a wild-type genomic *nmr-1* clone (green). Positive values and negative values represent a turn to the right or left, respectively (see Experimental Procedures for details). The dotted lines indicate the point of either 0.9 or −0.9 radians.

(B) The fraction of the total number of both left and right turns that are greater than an angle 0.9 radians. *Statistical difference from wild-type ($n = 10$, $p < 0.002$).

(C) The average duration of forward and backward movement on a food-free agar plate. Wild-type worms moved forward for an average duration of approximately 25 s ($n = 39$) before briefly reversing direction. *nmr-1(ak4)* worms moved forward for approximately 46 s ($n = 45$, $p < 0.001$) before reversing. The phenotype was rescued by a wild-type *nmr-1* genomic clone (*nmr-1[ak4; Ex58]*; $n = 39$, $p < 0.001$), but not by a frame-shifted version of this genomic clone (*nmr-1[ak4; Ex84]*; $n = 18$). The *nmr-1(ak4)* mutant phenotype was also rescued by the N-terminal GFP fusion (*nmr-1[ak4; Ex61]*; $n = 29$; $p < 0.001$), but was not rescued by the localization defective C-terminal fusion (*nmr-1[ak4; Ex1]*; n=44). *Statistical difference from wild-type.

(D) The average duration of forward and backward movement in wild-type worms, *nmr-1(ak4)* and *glr-1(ky176)* mutants, and the double-mutant *nmr-1(ak4);glr-1(ky176)*. The average duration of forward movement in *glr-1(ky176)* mutants ($n = 27$, $p < 0.001$) and the double mutant ($n = 26$, $p < 0.001$) were significantly different from wild-type. The forward duration of *glr-1(ky176)* and *nmr-1(ak4)* mutants was also significantly different from each other ($p < 0.03$) and from the double mutant (*glr-1[ky176]*, $p < 0.04$; *nmr-1[ak4]*, $p < 0.003$). *Statistical difference from wild-type.

(E) The durations of the forward times are fit by double exponential probability density functions. Forward time is the interval between successive backward movements. Data from (C) was fit with a two exponential distribution (see Experimental Procedures). For N2 (blue), $A_1 = 551$, $A_2 = 1038$, $\tau_1 = 17.43$ s, and $\tau_2 = 3.8$ s ($r^2 = 0.999$). For *nmr-1(ak4)* (red), $A_1 = 60.7$, $A_2 = 360$, $\tau_1 = 57$ s and $\tau_2 = 14.5$ s ($r^2 = 0.99$). These distributions are significantly different ($p < 0.001$).

(F) Standard deviation of the forward time plotted as a function of the mean forward time. Each point represents the data from a specific mutant or transgenic strain.

maze was constructed by painting lines of $CuSO_4$, a chemical that worms avoid, on a food-free agar plate (Figure 5A). Worms starting at one pole had to navigate through these repellant lines to reach, at the opposite pole, a point source of the attractant diacetyl (Bargmann et al., 1993). Within 2 hr, 50%–60% of wild-type worms reached the target spot of diacetyl (Figure 5B). In contrast, less than 25% of the *nmr-1(ak4)* mutants reached the target. This difference in maze performance was not due to differences in sensitivity to the sensory cues: wild-type and *nmr-1(ak4)* worms were equally repelled by $CuSO_4$ and were equally attracted to diacetyl when measured in the absence of $CuSO_4$ (Table 1). *nmr-1(ak4)* mutants that expressed a transgene encoding an *nmr-1* genomic clone were indistinguishable from wild-type worms in the maze assay, demonstrating that the maze chemotaxis defect was due to the deletion in *nmr-1* (Figure 5B). The defective chemotaxis to diacetyl by *nmr-1* mutants was apparent only when tested in the presence of the $CuSO_4$ barrier. The poor performance of *nmr-1(ak4)* mutants in the maze may be due to their altered regulation of forward movement. Like mutants on food-free agar plates, mutants in the maze showed a significant increase in the duration of forward movement compared with wild-type worms (Figure 5C).

The Localization of GLR-1 Is Independent of *nmr-1*

nmr-1 mutants, unlike *glr-1* mutants, show a normal response to nose touch, suggesting that GLR-1 expression and localization are not dependent on the activity of NMR-1. To test this hypothesis, we compared the distribution of a full-length GLR-1::GFP fusion protein

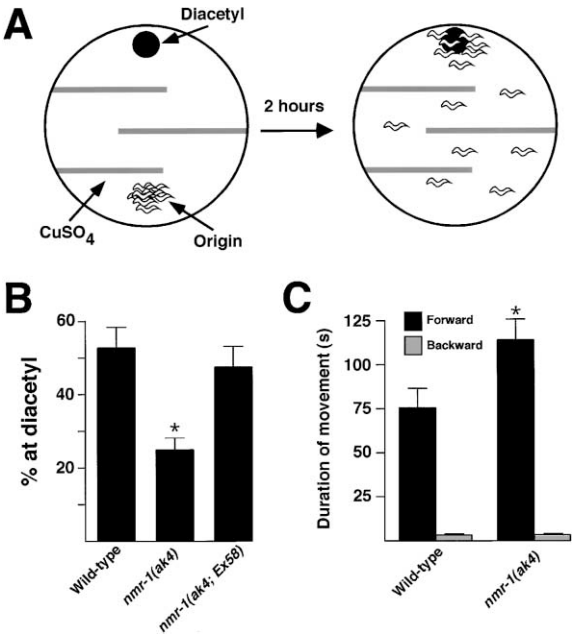

Figure 5. *nmr-1(ak4)* Worms Are Defective in Chemotaxis when Tested in a Maze Assay

(A) $CuSO_4$ barriers were staggered on a 10 cm agar plate as indicated (gray lines). Worms were placed at the origin and allowed 2 hr to move toward the volatile attractant diacetyl placed on the opposite side of the maze.

(B) After 2 hr, approximately 52% of the total number of wild-type worms had migrated to the diacetyl ($n = 22$). *nmr-1(ak4)* were less successful, with only 24% reaching the diacetyl ($n = 21$, $p < 0.001$). The phenotype was rescued by a wild-type *nmr-1* genomic clone (*nmr-1[ak4; Ex58]*).

(C) The average duration of both forward and backward movement of wild-type worms and *nmr-1(ak4)* mutants was determined as they moved through the maze. Compared with wild-type, *nmr-1(ak4)* mutants moved forward for significantly great periods of time before reversing direction ($n = 11$, $p < 0.03$). *Statistical difference from wild-type ($p < 0.05$).

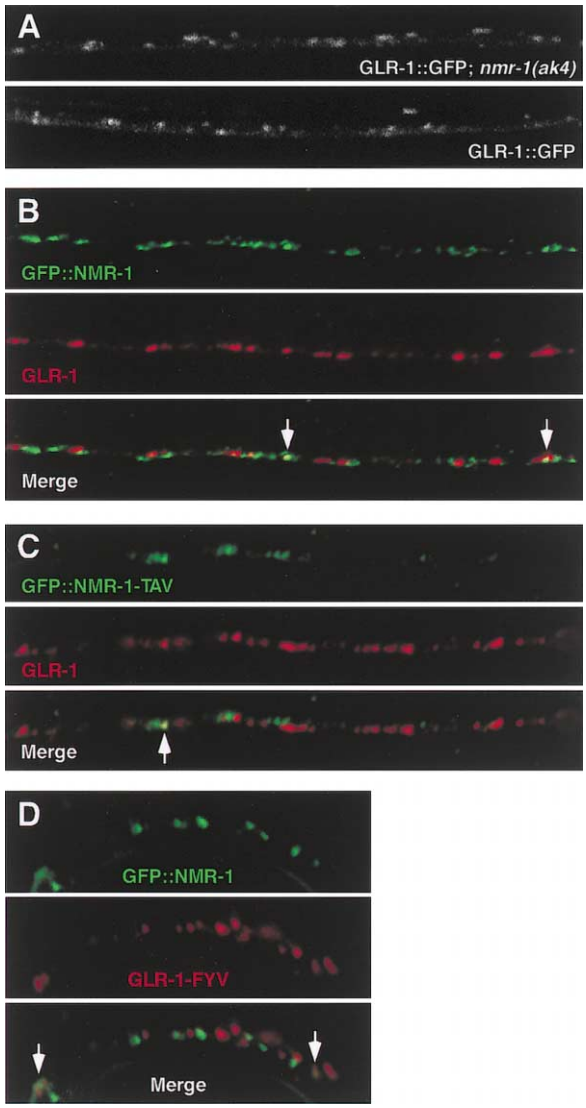

Figure 6. GLR-1 Localization Is Independent of NMR-1 and Shows Limited Colocalization with NMR-1

(A) Localization of GLR-1::GFP in *nmr-1(ak4)* mutants (top) and wild-type worms (bottom).

(B) Localization of GFP::NMR-1 (top) and GLR-1 (middle) detected using anti-GFP and anti-GLR-1 specific antibodies, respectively. Colocalization was observed at some sites indicated by arrows in the merged image (bottom).

(C) Localization of GFP::NMR-1-TAV (top) and GLR-1 (middle). Merged image (bottom).

(D) Localization of GFP::NMR-1 (top) and GLR-1-FYV (middle). Merged image (bottom). All images are of the processes of the ventral cord.

in wild-type and *nmr-1(ak4)* transgenic worms in the neural processes of the ventral cord. In the ventral nerve cord, GLR-1 and NMR-1 are expressed in the same subset of neurons save one. As shown previously (Rongo et al., 1998), in wild-type transgenic worms, the GLR-1::GFP fusion protein is localized to puncta that are believed to be synapses. When the same fusion protein is expressed in transgenic *nmr-1* mutants, neither the intensity nor the number of puncta appears modified (Figure 6A). These results suggest that localization of the non-NMDA receptor subunit GLR-1 is independent of NMR-1 activity.

NMR-1 and GLR-1 Are Differentially Localized

To determine whether NMR-1 and GLR-1 are localized to the same synapses, we used GLR-1-specific antibodies to examine the distribution of GLR-1 and GFP-specific antibodies to examine the distribution of the N-terminal GFP::NMR-1 fusion protein. Although we observed some overlap in the distribution of receptor-specific puncta (Figure 6B), for the most part, the receptors were differentially distributed. To determine whether clustering and segregation were dependent on the type II PDZ domain binding motif (FYV) found in NMR-1, we changed this motif to the type I PDZ domain binding motif (TAV) found in GLR-1 and expressed the modified receptor (GFP::NMR-1-TAV) in transgenic worms. The relative distributions of GFP::NMR-1 and GLR-1 did not appreciably change following the FYV/TAV exchange (Figure 6C). These results demonstrated that NMR-1 was expressed in a punctate distribution when tagged with either a type I or type II PDZ domain binding motif.

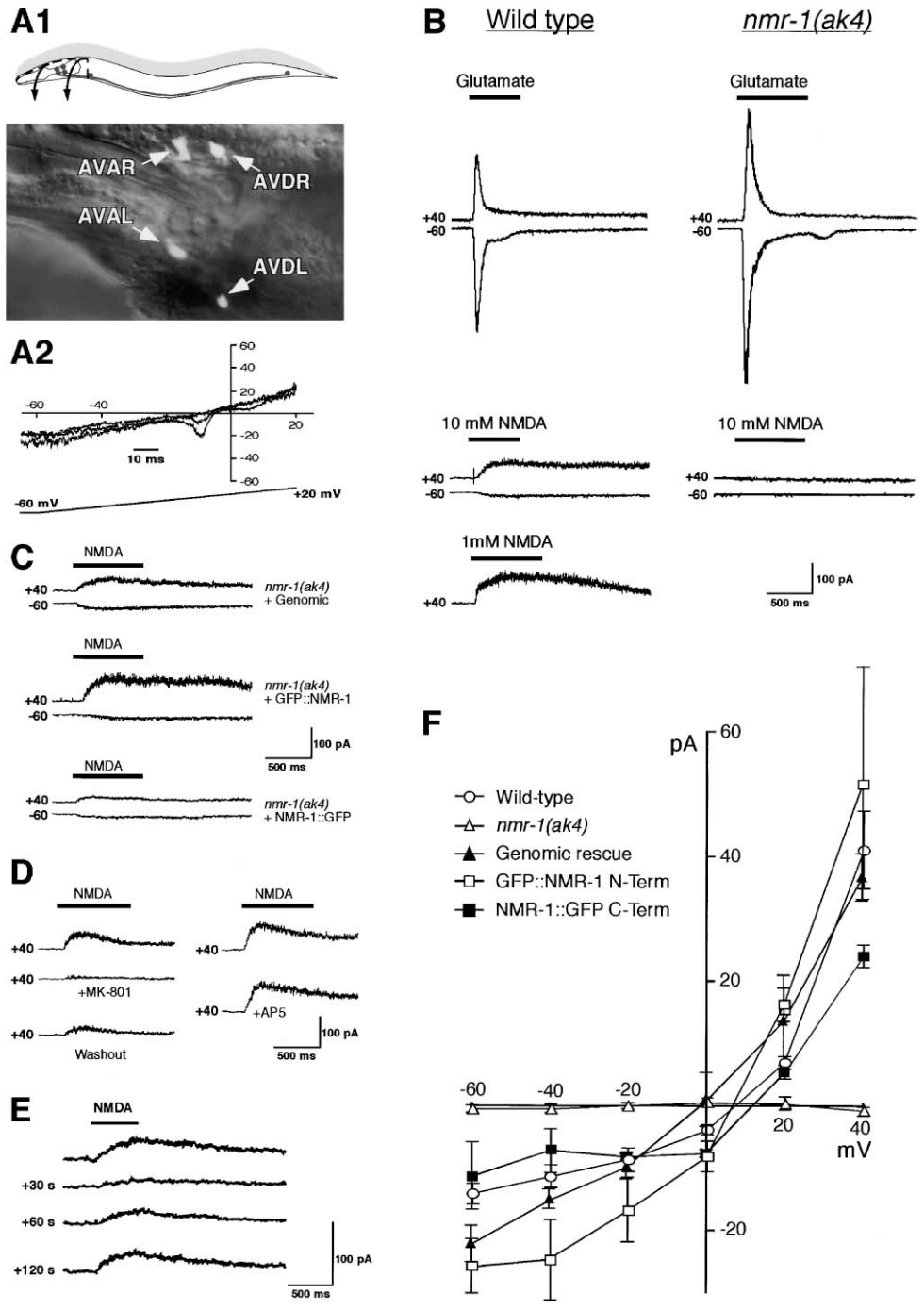

Figure 7. Electrophysiological Analysis of NMDA-Dependent Currents in Interneuron AVA

(A1) Exposed interneurons that express GFP. Pharyngeal region of the worm is shown in detail. The cuticle was peeled back and pinned to the coverslip exposing bilaterally symmetric pairs of interneurons. Electrical recordings were obtained from the AVA interneurons. To identify AVA, all strains contained an integrated transgene that expressed GFP under control of the *nmr-1* promoter.

(A2) Whole-cell recording protocol. Access to the interior was monitored by applying repeated voltage ramps applied to the pipette interior. As the membrane perforated due to the action of nystatin (see Experimental Procedures), whole-cell voltage-dependent membrane currents could be recorded.

(B) Glutamate and NMDA-dependent membrane currents from AVA in wild-type worms or *nmr-1(ak4)* mutants. The neuron was first clamped for 0.5 s to either +40 mV or −60 mV, and then a 0.5–0.75 s pulse of 1 mM glutamate was applied by pressure ejection from a closely placed pipette. In separate cells, either 10 mM or 1 mM NMDA was similarly applied.

(C) NMR-1-dependent currents are rescued in transgenic *nmr-1(ak4)* mutants. Current response to pressure application of 10 mM NMDA is shown. Genomic indicates a full-length genomic rescuing fragment. GFP::NMR-1 indicates a full-length N-terminal fusion protein to GFP. NMR-1::GFP indicates a full-length C-terminal fusion protein to GFP.

(D) Ten mM NMDA-dependent currents are blocked by the noncompetitive antagonist MK-801 but not by the competitive agonist AP5.

Conversely, when we changed the type I motif of GLR-1 to the type II motif (GLR-1-FYV), we again found that GLR-1 and GFP::NMR-1 were localized to distinct puncta (Figure 6D). Because GFP::NMR-1 and GLR-1 were differentially distributed, even when expressing the same PDZ domain binding motif, these binding motifs are probably not critical for directing receptors to specific synapses. Instead, they may have a role in clustering or stabilization of receptors once delivered to synapses.

NMDA-Activated Current in the Interneuron AVA Is Dependent on *nmr-1*

Deletion of *nmr-1* disrupts the pattern of locomotion and foraging ability. These defects may be associated with diminished or altered NMDA-dependent as well as non-NMDA-dependent glutamate-gated currents. To address the role of NMR-1 in synaptic function, we recorded glutamate-gated currents from the interneuron AVA. To expose interneurons that express *nmr-1::GFP*, we made a longitudinal slit along the head of the worm and then folded back the cuticle. Our recording preparation maintained the arrangement of neurons that expressed *nmr-1::GFP*, allowing identification of individual neurons (Figure 7A1).

Using patch-clamp recording techniques, we measured whole-cell currents from AVA (Figure 7A2). When the interneuron was held at −60 mV, pressure application of glutamate elicited a rapidly activating and inactivating inward current (Figure 7B). This current was also observed in *nmr-1(ak4)* mutants, demonstrating that the glutamate-gated current elicited at −60 mV was not substantially altered by the *nmr-1* deletion. The current amplitude varies from preparation to preparation, as can be seen in the small difference in glutamate-gated currents between *nmr-1* mutants and wild-type worms. The large, fast onset currents were not observed with application of 10 mM of the selective agonist NMDA, which at +40 mV elicited a slowly activating and inactivating outward current that was greatly reduced in amplitude in *nmr-1* mutants (Figure 7B). When the cell was held at −60 mV, application of NMDA elicited a small inward current in wild-type worms. The NMDA-dependent current was rescued in transgenic *nmr-1* mutants that expressed a wild-type *nmr-1* genomic construct (Figure 7C). NMDA-dependent currents were also restored in mutants that expressed either the localization-competent N-terminal GFP::NMR-1 fusion protein or the localization-defective C-terminal NMR-1::GFP fusion protein, indicating that incorrectly localized NMR-1 receptor subunits were competent to form functional receptors (Figure 7C).

NMDA receptors can be distinguished from non-NMDA receptors by the selective block by the noncompetitive antagonist MK-801 or the competitive antagonist 2-amino-5-phosphonopropionic acid (AP5). When AVA was bathed in 50 μM MK-801, the outward current elicited from a holding potential of +40 mV by application of 10 mM NMDA was almost eliminated (Figure 7D). This partial block was partly reversible with washout of the drug. In contrast, 100 μM AP5 had no appreciable effect on NMDA-evoked currents (Figure 7D). These results are consistent with the conservation of amino acids in NMR-1 known to be important for MK-801 binding (Ferrer-Montiel et al., 1995). However, many of the amino acids known to be required for AP5 binding are located on NR2 receptors (Anson et al., 1998; Laube et al., 1997), and these amino acids are not conserved in the NMR-2 receptor subunit (Brockie et al., 2001).

Another characteristic of NMDA receptors is desensitization, a time-dependent decrease in NMDA-dependent current that follows prolonged exposure to NMDA (Dingledine et al., 1999). We have found that NMR-1-dependent currents in AVA show prolonged desensitization to 10 mM NMDA. Full recovery of the current required approximately 2 min intervals between successive applications of NMDA (Figure 7E). Thus, in all experiments that required obtaining multiple current records, a 2.5 min interval was introduced between successive applications of NMDA.

Vertebrate NMDA receptors have a characteristic outward rectification that is dependent on a voltage-dependent block by Mg^{2+}. We found that NMDA-dependent currents in AVA were voltage dependent and exhibited a strong outward rectification (Figure 7F). This rectification was also observed in transgenic *nmr-1* mutants that expressed the localized and nonlocalized GFP fusion protein variants. We were not able to determine whether the rectification was dependent on the presence of extracellular Mg^{2+}. A reduction of external Mg^{2+} to a nominally zero level did not increase the NMDA-dependent current at negative holding potentials (data not shown). However, since AVA is still surrounded by adherent tissue, we could not ascertain how well the cell was perfused in situ. When we attempted to clamp Mg^{2+} to a low level by including mM quantities of the divalent cation chelator ethylenediaminetetraacetic acid in the external solution, the cell quickly became irreversibly leaky.

Expression of a Nondesensitizing Variant of GLR-1 Rescues the *nmr-1(ak4)* Phenotype

To test whether NMR-1 increases the probability of backward movement by virtue of its slow kinetics or its unique pore properties, we generated a variant of the GLR-1 subunit that approximates the kinetic properties of NMR-1-dependent receptors. We altered a conserved amino acid in GLR-1 previously shown to be important for desensitization of vertebrate non-NMDA receptors

Following bath application of MK-801, only a portion of the NMDA-dependent current was recovered following washout of the drug.
(E) Ten mM NMDA-dependent current shows prolonged desensitization following application of NMDA. Two applications of NMDA separated by either 30, 60, or 120 s times are shown. Between each set of applications was a 3 min recovery interval.
(F) Current-voltage relation for NMDA-dependent current in wild-type and transgenic *nmr-1(ak4)* mutants. Responses to glutamate were recorded in wild-type worms (n = 7), *nmr-1(ak4)* mutants (n = 6), and *nmr-1(ak4)* transgenic mutants that expressed either an *nmr-1* genomic clone (Genomic rescue; n = 2), an N-terminal GFP fusion (GFP::NMR-1 N-Term; n = 3), or a C-terminal GFP fusion (NMR-1::GFP C-term; n = 2). To identify the AVA interneurons, all strains also expressed GFP under control of the *nmr-1* promoter. SEM is indicated.

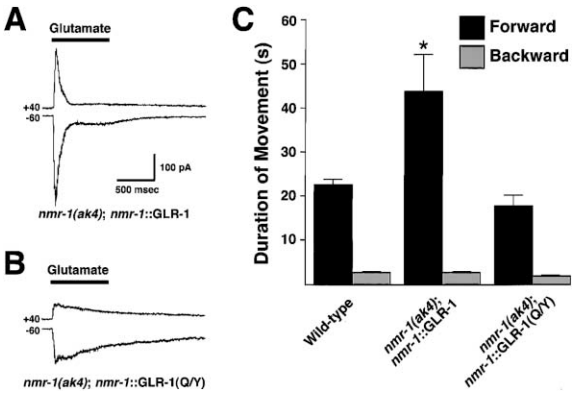

Figure 8. GLR-1(Q/Y) Can Compensate for the Loss of NMR-1

(A and B) Glutamate-gated currents recorded from the AVA interneuron in transgenic *nmr-1(ak4)* mutants expressing either GLR-1 (A) or the slowly desensitizing variant GLR-1(Q/Y) (B).

(C) The average duration of forward and backward movement in wild-type worms and transgenic *nmr-1(ak4)* mutants that expressed either GLR-1 or GLR-1(Q/Y) under the regulation of the *nmr-1* promoter. *Statistical difference from wild type ($p < 0.05$).

(Stern-Bach et al., 1998) and used the *nmr-1* promoter to express either the mutated receptor (GLR-1[Q/Y]) or wild-type GLR-1 in transgenic *nmr-1* mutants. Overexpression of GLR-1 did not appreciably alter either the kinetics or magnitude of the glutamate-gated current (Figure 8A). In comparison, overexpression of GLR-1(Q/Y) caused a dramatic slowing of desensitization such that the glutamate-gated currents had approximately the same time course as observed for NMDA-gated currents (Figure 8B). Interestingly, the fast component of the glutamate-gated current seen in wild-type worms was no longer observed, suggesting that GLR-1(Q/Y) is dominant and that most functional receptors contain GLR-1(Q/Y) (see Experimental Procedures). Overexpressing GLR-1(Q/Y), but not GLR-1, compensated for the loss of NMR-1 and rescued the *nmr-1(ak4)* mutant phenotype (Figure 8C). This result suggests that the kinetic properties, and not the pore properties, of NMR-1-dependent receptors are most important for the role of NMR-1 in modulating the probability of backward movement in *C. elegans*.

Discussion

A genetic analysis of NMDA receptors may help elucidate how these receptors are directed to particular synapses, how they function at synapses, and how their activity contributes to circuit function. Our analysis of NMR-1 in *C. elegans* revealed many interesting similarities and contrasts between NMDA receptors in *C. elegans* and vertebrates. NMR-1-dependent receptors share many of the pharmacological and kinetic properties of vertebrate NMDA receptors. In particular, the NMDA-gated currents are slow to activate and are long lived. However, some interesting differences are also apparent, as are some of the benefits of studying this receptor in *C. elegans*. First, NR1 is ubiquitously expressed in the vertebrate central nervous system (Dingledine et al., 1999), whereas NMR-1 expression in *C. elegans* is limited to a small subset of interneurons. Second, genetic disruption of the NR1 subunit in mice results in premature death (Forrest et al., 1994; Li et al., 1994). In contrast, *nmr-1(ak4)* mutants are viable and exhibit no gross developmental or behavioral defects. Third, the role of the C terminus of NR1 in receptor localization and function in vertebrates is unclear. In contrast, in *C. elegans*, it appears that disrupting the function of the PDZ domain binding motif of NMR-1 affects localization and behavior but not function of the receptor itself. Finally, in vertebrates, the insertion of certain glutamate receptor subunits is activity and NMDA receptor dependent (Shi et al., 1999), whereas the insertion of GLR-1 does not appear to be dependent on NMR-1 function. In fact, most neurons in *C. elegans* that express glutamate receptors do not express the NMR-1 receptor subtype (Brockie et al., 2001).

How Does the Locomotory Control Circuit Control Backward Locomotion?

Most organisms need to modulate dynamically the duration and direction of their movement to escape predation, to seek mates, and to forage for resources (in *C. elegans*, the term foraging has also been used to describe the movements of the worm's head; Kaplan and Horvitz, 1993). The circuits that control these behaviors are among the basic building blocks of all nervous systems. The locomotory control circuit is an example of such a circuit. How might NMR-1 function in this circuit to regulate the initiation of backward movement? Although the locomotory control circuit was first divided into forward and backward components with respect to touch sensitivity (Chalfie et al., 1985), it has been shown to have properties consistent with distributed function circuits (Zheng et al., 1999; Hart et al., 1995; Kristan et al., 1995). In this context, NMR-1 may be activated in forward and backward interneurons, yet act to bias the circuit to generate backward movements. Furthermore, we found that the intervals between backward movements are highly variable. This variability is believed to reflect, in part, correlated synaptic inputs. NMDA receptors widen the temporal window for the detection of correlated events and contribute to the variable output in a number of different neural circuits (Harsch and Robinson, 2000; Stevens and Zador, 1998).

As we have shown, a loss of NMR-1 function reduces the probability that a worm will switch from forward to backward directed movement. In the absence of NMR-1, sensory control may be less effective and the worm's movement more ballistic. In the maze assay, as opposed to standard chemotaxis assays, the worm is exposed to opposing stimuli, and constant modulation of forward and backward movement is required in order to reach the source of attractant. Thus, it is a more sensitive assay for defects in locomotion. Much like bacteria that extend favorable "runs" to reach a chemotactic target (Berg, 1975), worms may optimize their duration of forward movement in response to the complex stimuli that they encounter in their environs. Our results suggest that eliminating NMR-1 impairs a worm's ability to tailor effectively their movement to complex environmental stimuli.

Electrophysiological Analysis of Circuit Function in *C. elegans*

We have shown that NMR-1 containing receptors in the interneuron AVA contribute to long-lasting NMDA-activated currents that have many of the features of vertebrate NMDA-gated currents. These currents may act to amplify sensory responses and/or promote integration of temporally spaced inputs. We could test this possibility by expressing GLR-1(Q/Y), the nondesensitizing variant of GLR-1, in *nmr-1* mutants. By showing that GLR-1(Q/Y), but not wild-type GLR-1, could rescue the *nmr-1* mutant phenotype, we demonstrated that the kinetics of NMR-1 receptors, and not the pore properties, were crucial for modifying the probability of backward movement. NMR-1 may provide a possible mechanism to integrate sensory stimuli that arrive in a time window defined by the kinetics of the NMDA response. In one model, an individual sensory stimulus may not evoke a membrane potential change sufficient to cause a backward movement, but concurrent activation of multiple synaptic inputs could result in integration of these potential changes. Alternatively, sensory stimuli that signal at glutamatergic synapses may recruit NMDA receptors to inject additional currents into the synapse, providing amplification and increasing the probability of reversals. Both models depend on the long-lived currents provided by the NMDA receptor.

NMR-1 Receptor Subunits Appear to Be Localized to Specific Synapses

We have shown that localization of NMR-1 may be dependent on its PDZ domain binding motif and that overexpression of the localization-defective C-terminal NMR-1::GFP fusion protein was not sufficient for complete rescue of the *nmr-1(ak4)* mutant phenotype. Because we could still record NMDA-dependent currents from transgenic worms that expressed the mislocalized NMR-1 variant (Figure 7C), we could infer that functional NMDA receptors were present in the membrane. Localization of NMR-1 still occurred when we replaced the native type II PDZ domain binding motif with a type I motif. Irrespective of the specific binding motif, NMR-1 did not extensively colocalize with GLR-1, suggesting that the terminal PDZ domain binding motif does not direct receptors to specific synapses.

Mice that lack the C-terminal intracellular domain of NR2B die neonatally (Mori et al., 1998; Sprengel et al., 1998). Because a region of the intracellular domain is required for interaction with the PSD-95 family of PDZ domain proteins (Kornau et al., 1997), the truncated NR2B may not be localized to synapses, as was found in Mori et al. (1998). Alternatively, truncated NR2B may be localized to synapses and form functional channels but lack some other critical function, as found in Sprengel et al. (1998). In both studies, the deletion removed a large portion of the protein rather than specifically disrupting the predicted PDZ domain binding motif. Therefore, the significance of the PDZ domain for localization and function of NMDA receptors in vivo is still at issue in mice.

The different roles for GLR-1 and NMR-1 in the control of backward movement may reflect not only the different kinetics of their glutamate-gated currents but also the localization of GLR-1 compared with NMR-1. Although we have shown that GLR-1 and NMR-1 do not specifically colocalize, they may still be directed to different sites of the same synapse. Studies of glutamate receptors in retinal ganglion cells suggested that NMDA and non-NMDA receptors are differentially localized at the synapse (Matsui et al., 1998; Taylor et al., 1995). Thus, NMDA receptors were predicted to lie at peripheral sites of the synapse, making them less accessible to the released neurotransmitter. Activation of NMDA receptors, therefore, may rely on glutamate spillover from the release sites on bipolar cells. Bipolar cells, like neurons in *C. elegans*, transmit information via a graded potential that results in variable neurotransmitter release. By virtue of their peripheral location and long-lived currents, NMDA receptors on ganglion cells may function to integrate synaptic signals. We have shown that a similar organization of NMDA and non-NMDA receptors may also exist at synapses in *C. elegans*. If so, NMR-1 may have a small effect on the presumably large synaptic inputs associated with assays such as the nose touch response but still may contribute significantly to smaller correlated inputs. Thus, the contribution of NMR-1 to circuit function may vary depending on the strength or nature of the sensory input. These differences may also reflect the additive effect observed in the *nmr-1(ak4);glr-1(ky176)* double mutants.

We also showed that GLR-1 localization did not depend on the activity of NMDA receptors. We obtained indirect evidence for correct localization of GLR-1 in our behavioral experiments. The nose touch response, which requires localization of GLR-1 subunits (Rongo et al., 1998), is not disrupted in *nmr-1* mutants, suggesting that GLR-1 is localized in these mutants. When we examined the distribution of GLR-1::GFP, we noted no difference between wild-type worms and *nmr-1* mutants. Finally, the non-NMDA component of glutamate-gated currents did not appear altered in *nmr-1* mutants. These results suggest that the insertion and function of the non-NMDA receptor subunit GLR-1 are not dependent on NMR-1 and NMDA-gated currents.

In summary, we have used genetic techniques coupled with electrophysiological analysis to provide a detailed molecular analysis of neuronal and circuit function in *C. elegans*. We have shown that *nmr-1* encodes an NMDA receptor subunit that contributes to foraging behavior in *C. elegans*. We propose that the long-lived currents contributed by NMR-1-dependent receptors act to amplify or integrate sensory information and thus modify the probability of backward movements that function to reorient the worm.

Experimental Procedures

Molecular Biology

Cosmid F07F6 contains an open reading frame predicted to encode a NMDA receptor subunit (Wilson et al., 1994). The authentic 5′ end of *nmr-1* was identified by polymerase chain reaction using spliceleader SL1-specific oligonucleotides. The full-length NMR-1:GFP transgenes were constructed by the in-frame introduction of GFP coding sequences (A. Fire) immediately after the signal sequence (N-terminal fusion; pPB33) or immediately before the stop codon (C-terminal fusion; pPB10). pPB1 encodes a transcriptional fusion to GFP (Brockie et al., 2001). pPB65 encodes the nondesensitizing GLR-1(Q/Y) variant where site directed mutagenesis was used

to change the glutamine at position 552 of GLR-1 to a tyrosine. In each case, approximately 5 kb of *nmr-1* upstream sequence were included to drive expression. Other constructs include pCSW3, a genomic DNA fragment containing the *nmr-1* gene; pPB34, a frame-shifted version of pCSW3 that introduces a stop codon after amino acid 312; pV1, a wild-type *glr-1* genomic clone; pPB50, a variant of pV1 in which the last three codons of *glr-1* were modified to encode the type II PDZ domain binding motif −FYV; pPB56, a variant of pPB33 in which the last three codons of *nmr-1* were modified to encode the type I PDZ domain binding motif −TAV. A Tc1 transposon insertion in *nmr-1* was detected by polymerase chain reaction (Zwaal et al., 1993). Subsequently, a deletion mutation, *nmr-1(ak4),* was generated by imprecise excision of the transposon. *nmr-1(ak4)* was outcrossed 12 times to the wild-type N2 strain.

Transgenic Strains

As described previously, all transgenic strains were generated using microinjection to achieve germline transformation (Maricq et al., 1995). In all cases, *lin-15(n765ts)* mutants were injected with the *lin-15* rescuing plasmid (pJM23; 30 μg/ml), along with one of the following plasmids: pPB1, pPB10, pPB33, pPB34, pPB50, pPB56, pPB65, pCSW3, or pV1 (each at 70 μg/ml). Multiple independent extragenic lines were generated for each transgenic strain. Some transgenes were chromosomally integrated using psoralen mutagenesis and were repeatedly outcrossed. *nuIs25* (a gift from C. Rongo and J. Kaplan) is a transgenic line that expresses localized GLR-1::GFP fusion protein under the regulation of *glr-1* regulatory sequences.

Behavioral Assays

The duration of movement was measured as reported previously (Zheng et al., 1999). All of the strains that needed to be scored were randomized and scored on the same day. All movement assays were scored blind. Forward and backward durations reported throughout the text are mean ± SEM, and the significance of the differences was evaluated using the standard Student's t test. With worm velocity, body bends per minute were calculated by determining the number of body bends made during a 5 min period on a food-free agar plate. Body touch: anterior body touch was performed as described (Chalfie et al., 1985), and the number of body bends in response to the stimulus was determined. Osmotic avoidance: as previously described (Culotti and Russell, 1978), worms were placed in the center of a ring of 4 M fructose approximately 2 cm in diameter. After a 20 min period, the number of worms that had moved to the outside of the ring was calculated (% escaped). Nose touch: assays were performed by determining the number of responses to ten consecutive nose touch trials (% response) as previously described (Kaplan and Horvitz, 1993). Chemotaxis to diacetyl: standard chemotaxis assays were performed (Bargmann et al., 1993), and the specific Chemotaxis Index (C.I.) was calculated. C.I. = (the number of worms at attractant − the number of worms at counter attractant)/total number of worms. A C.I. of 1.0 indicates that all worms were attracted to the diacetyl, whereas a C.I. of −1.0 indicates that all worms were repulsed. $CuSO_4$ avoidance: assays were similar to those described for osmotic avoidance (Culotti and Russell, 1978), except that the worms were placed in the center of a ring of either 100 or 200 mM $CuSO_4$, and the percentage that escaped was determined after 1 hr. Defecation cycle: this describes the time interval (seconds) between consecutive defecation events. The maze assay was modified from the standard diacetyl chemotaxis assay (Bargmann et al., 1993) by painting three lines, 15 μl each, of 200 mM $CuSO_4$ and 1 μl of 1:1000 diacetyl at the positive pole. Approximately 100 worms were used in each maze assay. Of these, nearly 50% were not included in the analysis because they crawled onto the nearby walls and died. The percentage, corrected for the dead worms, at the diacetyl pole was evaluated at 2 hr. To determine the duration of directed movement in the maze, single worms were chosen at random and were scored after they had been moving through the maze for at least 30 min. Only worms that had moved around the first $CuSO_4$ barrier, but not the second barrier, were chosen. Worms were scored for 7 min, and the average duration of forward and backward movement was calculated. The significance of the findings was evaluated using the standard Student's t test.

Distribution of Turning Angles

Using motion sensitive software (DeltaVideo 2.0, Channel D, Red Bank, NJ), the paths of individual worms were monitored for 10 min following removal from food, with x-y coordinates of the worm recorded approximately once per second. This path was then rediscritized at the approximate body length of the worm (1.1 mm), and angles between sequential body lengths during the last 5 min of observation were taken as a measure of turns. Angles for ten worms of a given strain were then combined and used to generate Figure 4A. The figure is constructed by assigning a Gaussian distribution to each angle event and then summing the distributions and normalizing the sum to cover a total area of one (Splus 5 statistical software). The area between any two angles represents the probability that a turn within that range would be observed at any point during the period of observation.

Curve Fitting

Times between reversals were taken from Figure 4C. Using the maximum likelihood method, the distribution of forward times was found to fit a double exponential probability distribution significantly better than a single exponential ($P < 0.001$) for both N2 and *nmr-1 (ak4)*, but not significantly better than three exponentials. Using the method of maximum likelihood, the probability that the same exponential distribution describes N2 and *nmr-1(ak4)* is $p < 0.001$. Using a nonlinear least-squares algorithm, we fit the histograms in Figure 4E with the double-exponential distribution function, $A_1e^{(-t/\tau 1)} + A_2e^{(-t/\tau 2)}$, where τ_1 and τ_2 are the decay constants for the distributions. A_1 and A_2 represent the weights, and t represents the time between reversals. For N2, $A_1 = 551$, $A_2 = 1038$, $\tau_1 = 17.43$ s, and $\tau_2 = 3.8$ s. For *nmr-1(ak4)*, $A_1 = 60.7$, $A_2 = 360$, $\tau_1 = 57$ s, and $\tau_2 = 14.5$ s.

Electrophysiology

All recordings were from adult worms. The preparation of worms was similar to that previously described (Goodman et al., 1998). Worms were glued (Braun Histoacryl Blue) to glass coverslips coated with Sylgard. Using a fine glass needle, the cuticle was slit longitudinally along the length of the pharynx. To expose the neurons, a flap of cuticle was carefully retracted and pinned to the surface of the coverslip. To remove adherent tissue, dissected worms were rinsed in extracellular fluid (ECF) and then treated for 1 min with 1 mg/ml collagenase (Sigma Type IV) in ECF. Membrane currents were recorded at room temperature with tight-seal pipettes in the whole-cell configuration (Hamill et al., 1981), using a patch-clamp amplifier (EPC-9; HEKA Elektronik, Lambrecht, Germany) Whole-cell access was facilitated by incorporating the polyene antibiotic Nystatin in the pipette solution (Horn and Marty, 1988). The standard internal (pipette filling) solution contained K-gluconate (115 mM), KCl (25 mM), $CaCl_2$ (0.1 mM), HEPES (50 mM), MgATP (5 mM), Na-GTP (0.5 mM), Na-cAMP (0.5 mM), Na-cGMP (0.5 mM), and BAPTA (1 mM). The pH was 7.35 with KOH. Osmolarity was measured at 320 mOsm. The standard external solution contained NaCl (150 mM), KCl (5 mM), $CaCl_2$ (5 mM), $MgCl_2$ (1 mM), glucose (10 mM), HEPES (15 mM), glycine (20 μM). The pH was 7.35 with NaOH. Osmolarity was measured at 325–330 mOsm, adjusted with sucrose (0–5 mM).

Antibody Staining and Microscopy

To detect the expression and localization of GLR-1, GLR-1-FYV, GFP::NMR-1, and GFP::NMR-1-TAV, transgenic strains were generated by injecting *nmr-1(ak4);glr-1(ky176);lin-15(n765ts)* mutants with pJM23 (*lin-15* rescuing plasmid) and either pV1 (GLR-1) and pPB33 (GFP::NMR-1), pPB50 (GLR-1-FYV) and pPB33, or pV1 and pPB56 (GFP::NMR-1-TAV). Worms were prepared as described previously (Zheng et al., 1999). To detect either GLR-1 or GLR-1-FYV, affinity-purified rabbit polyclonal sera was used at a 1:200 dilution, and a Cy3-conjugated donkey anti-rabbit secondary antibody was used at 1:300 (Jackson Laboratories, West Grove, PA). To detect either GFP::NMR-1 or GFP::NMR-1-TAV fusion proteins, affinity-purified goat anti-GFP polyclonal sera was used at 1:50 dilution (Research Diagnostics, Inc., Flanders, NJ), and an Alexafluor 488-conjugated donkey anti-goat secondary antibody was used at 1:400 (Molecular Probes, Eugene, OR). Epifluorescence images were acquired using a Zeiss Axioskop microscope and a Princeton Instruments Micromax

CCD camera. Confocal images were acquired using a Zeiss LSM 510 Confocal Imaging System.

Acknowledgments

This research was supported in part by the Sloan Foundation, by support from the Burroughs Wellcome Foundation, by grant NS35812 from the National Institutes of Health, and by a University of Utah Graduate Research Fellowship (P.J.B.). We thank J.S. Parkinson, M. Vetter, and members of the Maricq laboratory for comments on the manuscript, D. Copenhagen for his insights into NMDA receptor function, C. Bargmann for assistance with cell identifications and helpful discussions, the *C. elegans* sequencing consortium for cosmid clones, C. Walker for help with the *nmr-1* genomic clone, C. Rongo and J. Kaplan for the gift of the *nuIs25* strain, T. Ishihara for the idea of pairing $CuSO_4$ with diacetyl, and T. Nickell for advice on obtaining perforated patches in *C. elegans*.

Received May 4, 2001; revised June 11, 2001.

References

Anson, L.C., Chen, P.E., Wyllie, D.J.A., Colquhoun, D., and Schoepfer, R. (1998). Identification of amino acid residues of the NR2A subunit that control glutamate potency in recombinant NR1/NR2A NMDA receptors. J. Neurosci. *18*, 581–589.

Bargmann, C.I., Hartwieg, E., and Horvitz, H.R. (1993). Odorant-selective genes and neurons mediate olfaction in *C. elegans*. Cell *74*, 515–527.

Berg, H.C. (1975). Bacterial behaviour. Nature *254*, 389–392.

Bourne, H.R., and Nicoll, R. (1993). Molecular machines integrate coincident synaptic signals. Cell Suppl. *72*, 65–75.

Brockie, P.J., Madsen, D.M., Zheng, Y., Mellem, J., and Maricq, A.V. (2001). Differential expression of glutamate receptor subunits in the nervous system of *C. elegans* and their regulation by the homeodomain protein UNC-42. J. Neurosci. *21*, 1510–1522.

Burnashev, N., Schoepfer, R., Monyer, H., Ruppersberg, J.P., Gunther, W., Seeburg, P.H., and Sakmann, B. (1992). Control by asparagine residues of calcium permeability and magnesium blockade in the NMDA receptor. Science *257*, 1415–1419.

Chalfie, M., Sulston, J.E., White, J.G., Southgate, E., Thomson, J.N., and Brenner, S. (1985). The neural circuit for touch sensitivity in *Caenorhabditis elegans*. J. Neurosci. *5*, 956–964.

Chalfie, M., Tu, Y., Euskirchen, G., Ward, W.W., and Prasher, D.C. (1994). Green fluorescent protein as a marker for gene expression. Science *263*, 802–805.

Croll, N.A. (1975). Components and patterns in the behaviour of the nematode *Caenorhabditis elegans*. J. Zool. Lond. *176*, 159–176.

Culotti, J.G., and Russell, R.L. (1978). Osmotic avoidance defective mutants of the nematode *Caenorhabditis elegans*. Genetics *90*, 243–256.

Dingledine, R., Borges, K., Bowie, D., and Traynelis, S.F. (1999). The glutamate receptor ion channels. Pharmacol. Rev. *51*, 7–61.

Ferrer-Montiel, A.V., Sun, W., and Montal, M. (1995). Molecular design of the N-methyl-D-aspartate receptor binding site for phencyclidine and dizolcipine. Proc. Natl. Acad. Sci. USA *92*, 8021–8025.

Forrest, D., Yuzaki, M., Soares, H.D., Ng, L., Luk, D.C., Sheng, M., Stewart, C.L., Morgan, J.I., Connor, J.A., and Curran, T. (1994). Targeted disruption of NMDA receptor 1 gene abolishes NMDA response and results in neonatal death. Neuron *13*, 325–338.

Goodman, M.B., Hall, D.H., Avery, L., and Lockery, S.R. (1998). Active currents regulate sensitivity and dynamic range in *C. elegans* neurons. Neuron *20*, 763–772.

Hamill, O.P., Marty, A., Neher, E., Sakmann, B., and Sigworth, F. (1981). Improved patch-clamp techniques for high-resolution recording from cells and cell-free patches. Pflugers Arch. *391*, 85–100.

Harsch, A., and Robinson, H.P. (2000). Postsynaptic variability of firing in rat cortical neurons: the roles of input synchronization and synaptic NMDA receptor conductance. J. Neurosci. *20*, 6181–6192.

Hart, A.C., Sims, S., and Kaplan, J.M. (1995). Synaptic code for sensory modalities revealed by *C. elegans* GLR-1 glutamate receptor. Nature *378*, 82–85.

Horn, R., and Marty, A. (1988). Muscarinic activation of ionic currents measured by a new whole-cell recording method. J. Gen. Physiol. *92*, 145–159.

Kaplan, J.M., and Horvitz, H.R. (1993). A dual mechanosensory and chemosensory neuron in *Caenorhabditis elegans*. Proc. Natl. Acad. Sci. USA *90*, 2227–2231.

Kornau, H.C., Seeburg, P.H., and Kennedy, M.B. (1997). Interaction of ion channels and receptors with PDZ domain proteins. Curr. Opin. Neurobiol. *7*, 368–373.

Kristan, W.B., Jr., Lockery, S.R., and Lewis, J.E. (1995). Using reflexive behaviors of the medicinal leech to study information processing. J. Neurobiol. *27*, 380–389.

Kuryatov, A., Laube, B., Betz, H., and Kuhse, J. (1994). Mutational analysis of the glycine-binding site of the NMDA receptor: structural similarity with bacterial amino acid-binding proteins. Neuron *12*, 1291–1300.

Laube, B., Hirai, H., Sturgess, M., Betz, H., and Kuhse, J. (1997). Molecular determinants of agonist discrimination by NMDA receptor subunits: analysis of the glutamate binding site on the NR2B subunit. Neuron *18*, 493–503.

Li, Y., Erzurumlu, R.S., Chen, C., Jhaveri, S., and Tonegawa, S. (1994). Whisker-related neuronal patterns fail to develop in the trigeminal brainstem nuclei of NMDAR1 knockout mice. Cell *76*, 427–437.

Malenka, R.C., and Nicoll, R.A. (1999). Long-term potentiation: a decade of progress? Science *285*, 1870–1874.

Malinow, R., Mainen, Z.F., and Hayashi, Y. (2000). LTP mechanisms: from silence to four-lane traffic. Curr. Opin. Neurobiol. *10*, 352–357.

Maricq, A.V., Peckol, E., Driscoll, M., and Bargmann, C.I. (1995). Mechanosensory signalling in *C. elegans* mediated by the GLR-1 glutamate receptor. Nature *378*, 78–81.

Matsui, K., Hosoi, N., and Tachibana, M. (1998). Excitatory synaptic transmission in the inner retina: paired recordings of bipolar cells and neurons of the ganglion cell layer. J. Neurosci. *18*, 4500–4510.

Mori, H., Manabe, T., Watanabe, M., Satoh, Y., Suzuki, N., Toki, S., Nakamura, K., Yagi, T., Kushiya, E., Takahashi, T., et al. (1998). Role of the carboxy-terminal region of the GluR epsilon2 subunit in synaptic localization of the NMDA receptor channel. Neuron *21*, 571–580.

Pierce-Shimomura, J.T., Morse, T.M., and Lockery, S.R. (1999). The fundamental role of pirouettes in Caenorhabditis elegans chemotaxis. J. Neurosci. *19*, 9557–9569.

Rongo, C., Whitfield, C.W., Rodal, A., Kim, S.K., and Kaplan, J.M. (1998). LIN-10 is a shared component of the polarized protein localization pathways in neurons and epithelia. Cell *94*, 751–759.

Schmidt, B.J., Hochman, S., and MacLean, J.N. (1998). NMDA receptor-mediated oscillatory properties: potential role in rhythm generation in the mammalian spinal cord. Ann. NY Acad. Sci. *860*, 189–202.

Seeburg, P.H., Burnashev, N., Kohr, G., Kuner, T., Sprengel, R., and Monyer, H. (1995). The NMDA receptor channel: molecular design of a coincidence detector. Rec. Prog. Horm. Res. *50*, 19–34.

Shi, S.H., Hayashi, Y., Petralia, R.S., Zaman, S.H., Wenthold, R.J., Svoboda, K., and Malinow, R. (1999). Rapid spine delivery and redistribution of AMPA receptors after synaptic NMDA receptor activation. Science *284*, 1811–1816.

Sigvardt, K.A., Grillner, S., Wallen, P., and Van Dongen, P.A. (1985). Activation of NMDA receptors elicits fictive locomotion and bistable membrane properties in the lamprey spinal cord. Brain Res. *336*, 390–395.

Sillar, K.T., and Simmers, A.J. (1994). 5HT induces NMDA receptor-mediated intrinsic oscillations in embryonic amphibian spinal neurons. Proc. R. Soc. Lond. B Biol. Sci. *255*, 139–145.

Songyang, Z., Fanning, A.S., Fu, C., Xu, J., Marfatia, S.M., Chishti, A.H., Crompton, A., Chan, A.C., Anderson, J.M., and Cantley, L.C. (1997). Recognition of unique carboxyl-terminal motifs by distinct PDZ domains. Science *275*, 73–77.

Sprengel, R., Suchanek, B., Amico, C., Brusa, R., Burnashev, N.,

Rozov, A., Hvalby, O., Jensen, V., Paulsen, O., Andersen, P., et al. (1998). Importance of the intracellular domain of NR2 subunits for NMDA receptor function in vivo. Cell *92*, 279–289.

Stern-Bach, Y., Bettler, B., Hartley, M., Sheppard, P.O., O'Hara, P.J., and Heinemann, S.F. (1994). Agonist selectivity of glutamate receptors is specified by two domains structurally related to bacterial amino acid-binding proteins. Neuron *13*, 1345–1357.

Stern-Bach, Y., Russo, S., Neuman, M., and Rosenmund, C. (1998). A point mutation in the glutamate binding site blocks desensitization of AMPA receptors. Neuron *21*, 907–918.

Stevens, C.F., and Zador, A.M. (1998). Input synchrony and the irregular firing of cortical neurons. Nat. Neurosci. *1*, 210–217.

Tang, Y.P., Shimizu, E., Dube, G.R., Rampon, C., Kerchner, G.A., Zhuo, M., Liu, G., and Tsien, J.Z. (1999). Genetic enhancement of learning and memory in mice. Nature *401*, 63–69.

Taylor, W.R., Chen, E., and Copenhagen, D.R. (1995). Characterization of spontaneous excitatory synaptic currents in salamander retinal ganglion cells. J. Physiol. *486*, 207–221.

Tsien, J.Z., Huerta, P.T., and Tonegawa, S. (1996). The essential role of hippocampal CA1 NMDA receptor-dependent synaptic plasticity in spatial memory. Cell *87*, 1327–1338.

Viana Di Prisco, G., Ohta, Y., Bongianni, F., Grillner, S., and Dubuc, R. (1995). Trigeminal inputs to reticulospinal neurones in lampreys are mediated by excitatory and inhibitory amino acids. Brain Res. *695*, 76–80.

White, J.G., Southgate, E., Thomson, J.N., and Brenner, S. (1986). The structure of the nervous system of the nematode *Caenorhabditis elegans*. Phil. Trans. Roy. Soc. (Lond.) B *314*, 1–340.

Wilson, R., Ainscough, R., Anderson, K., Baynes, C., Berks, M., Bonfield, J., Burton J, Connell, M., Copsey, T., Cooper, J., et al. (1994). 2.2 Mb of contiguous nucleotide sequence from chromosome III of *C. elegans*. Nature *368*, 32–38.

Zheng, Y., Brockie, P.J., Mellem, J.E., Madsen, D.M., and Maricq, A.V. (1999). Neuronal control of locomotion in *C. elegans* is modified by a dominant mutation in the GLR-1 ionotropic glutamate receptor. Neuron *24*, 347–361.

Zwaal, R.R., Broeks, A., van Meurs, J., Groenen, J.T., and Plasterk, R.H. (1993). Target-selected gene inactivation in *Caenorhabditis elegans* by using a frozen transposon insertion mutant bank. Proc. Natl. Acad. Sci. USA *90*, 7431–7435.